DESGIGN PARAMETERS OF THE NORMAL CONDUCTING BOOSTER CAVITY FOR THE PITZ-2 TEST STAND

V.V. Paramonov, N.I. Brusova, A.I. Kvasha, A.A. Menshov, O.D. Pronin,
A.K. Skasyrskaya, A.A. Stepanov, INR, 117312 Moscow, Russia
A. Donat, M. Krasilnikov, A. Oppelt, F. Stephan, DESY, Zeuthen, Germany
K. Floettmann, DESY, Hamburg, Germany

Abstract

The normal conducting booster cavity is intended to increase the electron bunch energy in the Photo Injector Test (DESY, Zeuthen) stage 2 experiments [1]. The normal conducting cavity is selected due to infrastructure particularities in DESy Zeuthen. The L-band cavity is designed to provide the accelerating gradient up to 14 MV/m with the total input rf power up to 8.6 MW, rf pulse length up to 900 mks and repetition rate 5 Hz. The multi-cell cavity is based on the CDS compensated accelerating structure with the improved coupling coefficient value. The main design ideas and decisions are described briefly together with cavity parameters - rf properties, cooling and pumping circuits.

GENERAL PARAMETERS

Table 1: Cavity parameters

Parameter	Unit	Value
Operating frequency	MHz	1300
Particle velocity	relative	1.0
Nominal gradient E_0T	$\frac{MV}{m}$	12.5
Maximal gradient E_0T	$\frac{MV}{m}$	14.0
Nominal energy gain	MeV	20.18
Maximal surface field	$\frac{MV}{m}$	40.0
Maximal rf pulse power	MW	8.6
Maximal rf pulse length	μks	900
Nominal repetition rate	Hz	5
Aperture diameter	mm	30.0
Number of periods		14
Coupling coefficient	%	7.2
Calculated Q-factor		23700
Required Q-factor	at $20C^o$	20100
Cavity length	m	≈ 1.8
Operating temperature	C^o	≈ 44
Cooling water consumpt.	$\frac{m^3}{h}$	4.5
Residual gas pressure	$Torr$	$\leq 10^{-7}$

The booster cavity is the component of the test stand for investigations of high brightness electron beam formation. The cavity should combine different, some time contradictory, properties as operating parameters flexibility, reliability, minimal own emittance perturbations. Additionally the cavity realize (in maximal parameters) the full scale high power prototype of the high gradient cavities in the TESLA Positron Pre-Accelerator [2].
The cavity general parameters are summarized in Table 1.

Accelerating structure and beam dynamics

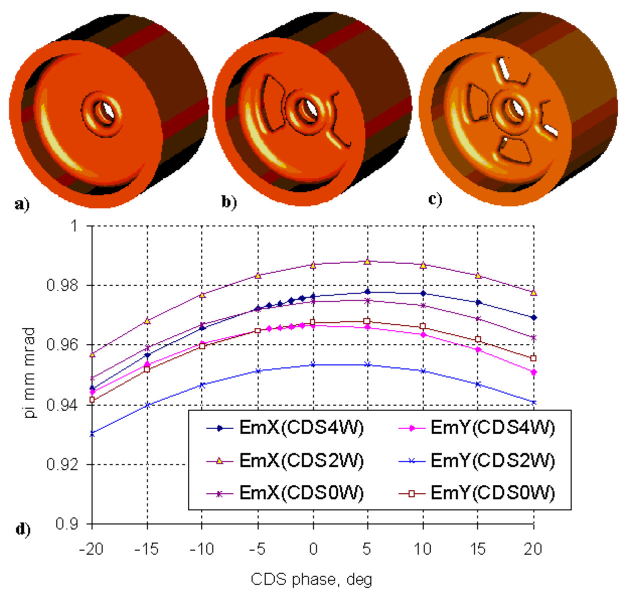

Figure 1: Top - the structure options for BD investigations, a) - axial symmetrical (CDS0W), b) - with two (CDS2W) and c) with four coupling windows. Bottom - d) the transverse rms beam emittance for different CDS options.

The cavity should provide the maximal energy gain for the maximal gradient $E_0T = 14\frac{MV}{m}$ with input rf power $P_i = 8.6MW$ and the structure effective shunt impedance Z_e should be reasonably optimized. The CDS structure [3], which combines improved coupling coefficient k_c, high Z_e value and small dimensions, is chosen. The options with two (CDS2W), Fig. 1b, and four (CDS4W), Fig. 1c, were considered. The axially symmetric option (CDS0W), Fig. 1a, is used as a reference. The moderate, not maximal possible, k_c values, $k_c^{2W} = 9.55\%$ and $k_c^{4W} = 7.2\%$, are chosen to obtain higher Z_e values, which are $Z_e^{2W} = 0.995Z_e^{0W}$ and $Z_e^{4W} = 1.03Z_e^{0W}$ (calculated values). To have higher Z_e value, the coupling windows edges - the place of maximal rf current density - are rounded. It leads to higher sensitivity of k_c value on win-

dows dimensions (and rounding radius) deviations, but we consider the achieved Z_e rise $\approx 5\%$ as more important.
The emittance perturbation by the cavity should be minimal. The beam dynamics simulations, taking into account space charge and real 3D fields maps, have performed by using ASTRA code [4]. The plots of transverse rms emittance as the functions of the phase difference between rf gun and CDS booster are shown in Fig. 1d. The visible quadruple addition in the magnetic field distribution near axis was founded for CDS2W option. Nevertheless, for small nominal relativistic ($\gamma > 10$) beams the difference in rms emittance between different CDS option is very small and beam dynamics requirements is not a point for the structure option definition.
The CDS2W option is more simple for construction, but due to:
- higher shunt impedance value;
- higher vacuum conductivity;
- more uniform field distribution in the aperture;
- more effective cooling circuit,
the CDS4W option has been adopted for the booster cavity.

CAVITY DESIGN

The cavity general view is shown in Fig. 2. The cavity has 11 regular CDS4W cells, rf coupler cell and two end cells. Each regular cell has 8 bind holes for frequency tuning after cavity final brazing by wall deformation.
Two rf probes (Fig. 2 - 4) are intended for direct rf phase

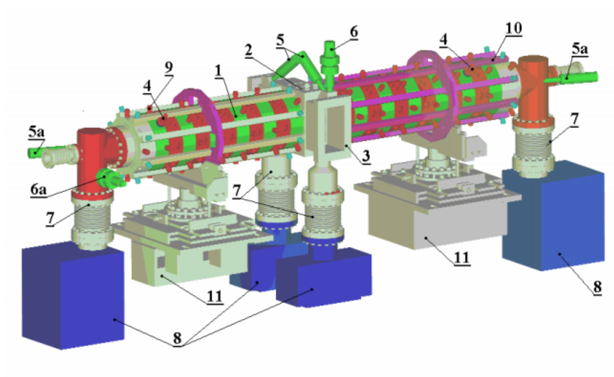

Figure 2: Booster cavity. 1 - regular cells, 2 - rf coupler cell, 3 - rf connecting flanges, 5 - photo multipliers, 5a - reserve photo multipliers, 6 - vacuum gauge, 6a- reserve vacuum gauge, 7 - pumping tubes with bellows, 8 - ion pumps, 9 - internal cooling circuit outlets, 10 - outer cooling circuit, 11 - support and adjuctment.

measurements in the cavity. As shows the rf gun experience, the Photo-Multiplier (PM) is the mostly fast and sensitive sensor to detect sparking and electric breakdowns in the rf gun cavity. Two PMs, one for each ceramic window, are foreseen in the rf coupler cell, Fig. 2 - 5. The CDS structure is not so transparent optically, as rf gun cavity. Two additional PMs are foreseen, for safety, at the cavity ends (Fig. 2 - 5a) - may be a problems, related to X-rays flux along the cavity axis.

RF coupler

RF coupler cell (Fig. 2 -2)is the most complicated part of the cavity and comprises a lot of contradictory requirements. The cavity will be driven with standard TESLA $10MW$ klystron, which is designed with two output windows. Due to a lot of reasons, the symmetrical rf coupler, Fig. 3, is adopted for CDS booster. Such coupler provides minimized oqtupole field perturbations. One half of the total rf power ($\approx 4.3MW$) will be transmitted through each coupler shoulder, allowing the applications of well tested $5MW$ ceramic rf windows. To minimize the electric field value at matching slots, the inductive type slots (Fig. 3 - 2) are chosen. The slots rounding, together with slots cooling, is foreseen to reduce the maximal rf current density and keep the surface temperature within limits $T_{max} < 45C^o$. The preliminary estimations for matching slots dimension were done following [5].
To meet requirements of matching and frequency tuning,

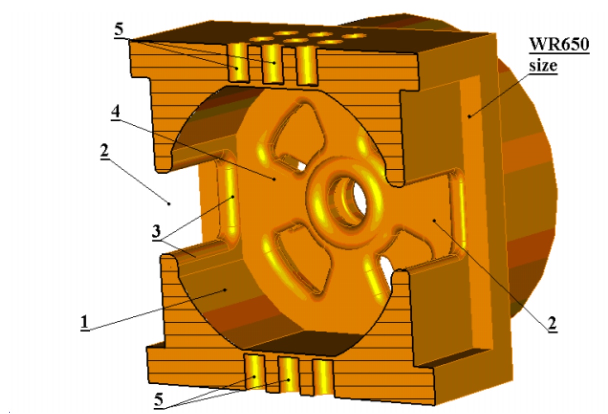

Figure 3: Symmetrical rf coupler. 1 - rf coupler cell, 2 - matching slots, 3 - rounding, 4 - diaphragm, 5 - blind holes.

reasonable construction, the rf coupler cell has a simplified shape (Fig. 3 - 1) with Z_e value $\approx 10\%$ lower as compared to regular CDS4W cells. Straight plates are foreseen for matching slots placing, Fig. 3 - 2, to simplify matching condition tuning, and for operating frequency tuning. Preliminary frequency tuning, before the cell brazing, is foreseen by material removal from straight parts. For fine narrow range frequency tuning after cavity brazing, 18 blind holes (Fig. 3 - 5) are used for reversible ($\pm\delta f_a$) tuners, developed and tested at the PITZ rf gun.

Pumping and cooling circuits

The own vacuum conductivity of the CDS4W structure is estimated as $\approx 300\frac{l}{sec}$ with main contribution due to coupling windows configuration. Four pumping ports are foreseen in the cavity (Fig 2 - 7, 8) - at the each cavity end (with Varian Vacion 150 pumps) and two in the middle of the cavity - through rf grids in the waveguide shoulders of rf coupler - with Vacion 75 pumps. To improve the vacuum conductivity of the end cells, four narrow radial slots are in the end wall, simultaneously compensating partially the oqtupole field perturbation from the coupling windows at opposite wall of the end cells.

Assuming the out-gassing rate $q_g \approx 7 \cdot 10^{-11} \frac{Torr \cdot l}{sec}$ after cavity rf conditioning, the maximal residual gas pressure is expected as $\approx 8 \cdot 10^{-9} Torr$. This pumping scheme has a good reliability and the maximal pressure $\approx 1 \cdot 10^{-7} Torr$ is expected even for simultaneous failure of two pumps.

The residual pressure value can be estimated by measuring the pumps currents. Additionally one vacuum gauge is foreseen in rf coupler shoulder (Fig. 2 - 6) for direct pressure measurement. Additional gauge, Fig. 2 - 6a, is recommended at the cavity end, closer to rf gun (vacuum requirements for rf gun are more severe).

The maximal average rf power, dissipated in the cavity, is $38.7kW$, or $\approx 2.8kW$ per structure period. To keep the surface temperature reasonably low, both drift tube region, and outer wall cooling are required. The cooling scheme (Fig. 4a) has two circuits - for for regular cells webs internal cooling, Fig. 4a - 1, and for outer one, Fig. 4a -2. Inside each circuit several channels are connected in series in groups and groups are connected in parallel. The flow velocities in circuits are chosen (and are in safe limits - $\approx 1.8 \frac{m}{sec}$ and $\approx 2.1 \frac{m}{sec}$) to have the same temperature rise ($\approx 7C^o$), providing the most efficient conditions for cavity cooling. The thermal-stress analysis has been performed following [6]. The expected temperature distribution at the cell surface for maximal power, assuming the input water temperature $30C^o$, is shown in Fig. 4b, corresponding to frequencies shifts $\approx -270kHz$ for the operating mode and $\approx -105kHz$ for the coupling one, taking into account the cooling water temperature rise. The equivalent cavity temperature increasing, with respect input water temperature, is $\approx 13C^o$.

For the adopted cooling scheme the maximal internal

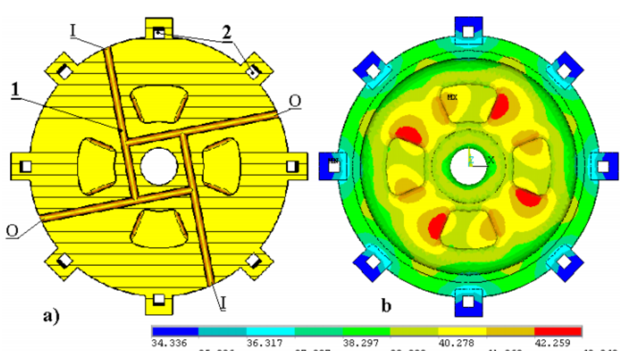

Figure 4: The cooling scheme (a) and temperature distributon (b) for regular cells. 1 - internal channels, 2 - external circuit.

stress, due to non uniform cells rf heating, are well inside safe limit - three times less than yield stress for OFC copper.

CAVITY TECHNOLOGY

For higher operational reliability the cavity is designed as the totally brazed device. RF contacts with vacuum sealing are used just at the flange (Fig. 2 - 3) for connection with $5MW$ rf ceramic input windows. This case we use the same flange design as tested at rf gun cavity.

The standard solution - one structure period consists from two half-cells - is adopted for regular cells. The cavity material is the OFC copper Class 1. For higher vacuum reliability the cooling circuits design has been performed to avoid all 'water - vacuum' brazed joints. it is the reason for non symmetric internal cooling channels scheme, Fig. 4a.

The surface roughness is specified as $R_a \sim 0.1 \mu km$ at the drift tube noses, to decrease the possible dark current field emission. For lathe treated parts of the cell surface the requirements $R_a \sim 0.2 \mu km$ and for milling reated parts (coupling windows) - $R_a \leq 0.4 \mu km$. With such requirements to the surface roughness for the totally brazed cavity after rf tuning we expect the cavity quality factor 85% from the calculated one.

The tolerances for cell dimensions were fixed following to the procedure [7] to have the relative rms field deviation $\sigma_E \leq 1\%$. The booster cavity is not too long and coupling coefficient deviations define mainly σ_E value. Both the requested tolerances $\pm(20 \div 50) \mu km$ and the surface roughness are not a problem for present technology.

The cavity will be constructed by DESY Hamburg in cooperation with industry. The construction begins now with the plan to have the conditioned cavity in the 2005 end.

ACKNOWLEGMENTS

The authors thank a lot of people both in INR and in DESY, both in Zeuthen and Hamburg, for valuable discussions, comments, proposals and support of this development.

REFERENCES

[1] A. Oppelt et al., Future plans at the Photo Injector Test Facility at DESY Zeuthen. Proc. of the 2003 FEL Conference, 18-23 September, Tsukuba, Japan, 2003

[2] K. Flottmann, V. Paramonov (ed.) Conceptual design of a positron injector for the TESLA linear collider. TESLA report 2000-12, Hamburg, DESY, 2000.

[3] V.V. Paramonov, The Cut Disk Structure for High Energy Linacs, Pros. 1997 PAC, v.3, p. 2962. 1998.

[4] K. Floettmann. ASTRA user guide, `www.desy.de/~mpflo/ASTRA_documentation`

[5] S. Kurennoy, L. Young. RF coupler for high-power CW FEL photoinjector. Proc. of the 2003 PAC, p. 3515, 2003

[6] S.C. Joshi, V.Paramonov et. al., The complete 3D coupled RF-Thermal-Structural-RF analysis procedure for a normal conduction accelerating structure for high intensity hadron linac. Proc. of the 2002 Linac Conference, p. 218, 2003

[7] V. Paramonov, A. Skasyrskaya. The technique for the numerical tolerances estimations. THP90, this Conference.